ISSN 1029-9599, Physical Mesomechanics, 2013, Vol. 16, No. 2, pp. 162–169 © Pleiades Publishing, Ltd., 2013.
Original Russian Text © M.E. Kozhevnikova, 2012, published in Fizicheskaya Mezomekhanika, 2012, Vol. 15, No. 6, pp. 59–66.

Plastic Zone Boundary and Poisson's Ratio Depending on Plastic Loosening

M. E. Kozhevnikova

Lavrentiev Institute of Hydrodynamics, Siberian Branch, Russian Academy of Sciences, Novosibirsk, 630090 Russia
m.e.kozhevnikova@yandex.ru

Received July 13, 2012

Abstract—A more accurate determination of the plastic zone boundary for plane strain and plane stress state is proposed. The plastic zone boundary is determined with regard to plastic loosening, given exact stress distribution and Schleicher yield criterion. The presence of mean normal stress in the Schleicher criterion ensures uniform expansion of the plastic zone. The dependence of Poisson's ratio and constraint ratio for plastic strain on plastic loosening of material is examined. These parameters peak at the tip or in the immediate vicinity of a stress concentrator and decrease with distance from it. In a small neighborhood of the crack tip, a region is found in which Poisson's ratio is impossible to determine from the Schleicher criterion. The size of this region is identified with the size of the region of exhausted plasticity.

DOI: 10.1134/S1029959913020070

Keywords: Schleicher criterion, plastic loosening, plastic zone, Poisson's ratio.

1. METHODS OF NONEQUILIBRIUM DYNAMICS AND FRACTURE MECHANICS USED IN COMBINATION TO FIND GENERAL MECHANISMS OF PLASTIC DEFORMATION

In recent years much attention has been paid to the study of general mechanisms of plastic deformation and fracture of solids on the basis of nonequilibrium thermodynamics. According to the thermodynamic approach all types of strain-induced defects are nucleated in local zones of hydrostatic tension near stress concentrators, where the dependence of local nonequilibrium thermodynamic Gibbs potential $F(v)$ on molar volume v of the loaded material should be considered [1]. As a rule, ductile metals under loading demonstrate all intermediate maxima of the Gibbs potential shown in Fig. 1. Consequently, metal crystals in tension reveal the entire sequence of strain-induced defects, namely, dislocations, meso- and macrobands of localized deformation, material fragmentation, micropore formation, and propagation of the main crack in the local zone of a stress macroconcentrator [2, 3]. Deformation and fracture zones of solids shown in the diagram for thermodynamic potential $F(v)$ versus molar volume v are thoroughly studied and consequently regions of applicability for the basic principles of fracture mechanics are found. The diagram in Fig. 1 exhibits the following regions [1]:

– $v < v_{-1}$ is the region of hydrostatic compression characterized by incompressibility of a solid;

– $v_{-1} - v_1$ is the region of elastic compression-tension of an equilibrium crystal;

– $v_1 - v_4$ is the region of plastic deformation of a solid without signs of destruction of the defective material and without a possibility of complete restoration of its equilibrium, which is related to the development of meso- and macrobands of localized deformation. The evolution of band structures ends in material fragmentation. Between fragments of the crystalline material a "quasi-amorphous phase" is formed, that experiences hydrodynamic flow;

– $v_4 - v_6$ is the region of formation of different-scale discontinuities, micropores, and cracks. Such defects can arise only in local zones of hydrostatic tension, which are characterized by increasing molar volume.

On the interval $v_{-1} - v_4$, where $F(v) < 0$, any defective phase is nonequilibrium and in a thermodynamic sense retains the capability to pass to the equilibrium

crystalline state. On the interval $v_4 - v_6$, where $F(v) > 0$, the crystal presents an atom-vacancy structure with abnormally high nonequilibrium molar volume.

Most elastic-plastic models of the fracture mechanics are developed on the assumption of the material incompressibility. Formally processes described by these models should correspond to variations occurring in local zones of stress macroconcentrators, where hydrostatic compression occurs. Such zones are defined on the deformation interval $v_{-1} - v_1$ in the $F(v)$ diagram. However, judging from the associated flow rule any plastic deformation should be accompanied by a monotonous increase in volume, that can be physically explained by the micropore formation in the body, i.e., by plastic loosening [4]. Consequently, attention should be paid to the interval $v_4 - v_6$ characterized by hydrostatic tension, where the assumption of the material incompressibility is irrelevant.

Nevertheless, most applied problems of the fracture mechanics are solved on the assumption of material incompressibility because of both mathematical difficulties and lack of knowledge on the strain-dependent behavior of Poisson's ratio. A number of simplifications are therewith assumed to validate the hypothesis of material incompressibility. Plastic strains are thought, as a rule, to be much higher than elastic ones. With the volume strain being a quantity of an order of magnitude of elastic expansion, the volume is assumed to vary negligibly under plastic deformation. This statement allows introducing the hypothesis of material incompressibility at the plastic stage of deformation. Whence it follows that at the plastic stage of deformation the Poisson's ratio takes the value $\nu = 0.5$, which bears good agreement with the experimental data.

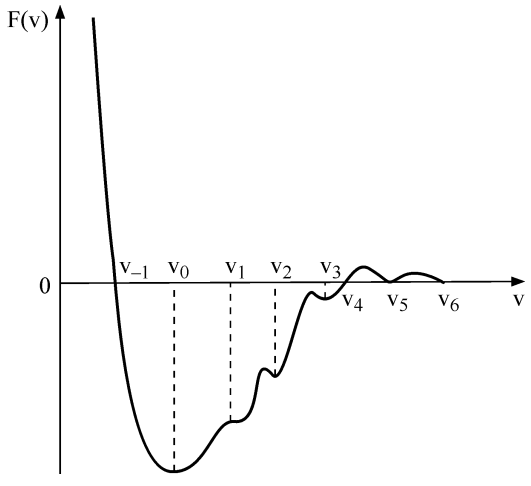

Fig. 1. Thermodynamic Gibbs potential $F(v)$ versus molar volume v with consideration for local zones of stress concentrators of different scale [1].

In fact, Poisson's ratio variation with increasing plastic strains is confirmed by numerous experiments on simple tension. Stang, Greenspan, Newman [5] carried out a tensile test of annealed specimens from low-carbon steel and obtained the Poisson's ratio increase up to 0.43...0.44. By measuring the density of deformed (up to 10%) and undeformed specimens from 40 and 45 grade steels, Davidenkov and Vasil'eva [6] found that the Poisson's ratio achieves 0.47. Zhukov [7] performed simple tensile tests for solid cylinder specimens from 40 and 45 grade steel and aluminum and stated that under plastic deformation the Poisson's ratio differs from 0.5 by less than 10%.

Note that the hypothesis on material incompressibility works fine as according to the experiments the volume variation does not exceed 0.5%. However, with all undeniable advantages it gives no consideration to such effect as plastic expansion. Though, in fact, this effect is true. Judging from the experiments (for example, [8]), at first (at plastic strains less than 1...2%) the effect of boundary translation prevails and then boundary expansion takes on primary meaning.

Thus, at a certain stage the plastically deformed material experiences plastic expansion, during which Poisson's ratio is registered to increase to $\nu = 1/2$. However, as in this case the material cannot be incompressible any more, the coefficient ν cannot be constant and equal to $1/2$ within the whole plastic zone.

The present paper proposes a more accurate determination of the plastic zone boundary for an internal mode I crack in case of plane strain and plane stress state. The plastic zone boundary is determined on the basis of exact stress distribution and Schleicher yield criterion (Schleicher criterion specifies Mises criterion with consideration for plastic loosening). We also study how Poisson's ratio varies within this zone with distance from a stress concentrator.

2. STRESS STATE IN AN INITIALLY CRACKED PLATE FOR PLANE STRAIN AND PLANE STRESS STATE

Let us determine the stress state at an arbitrary point of a cracked plate. The stress tensor components for the plate with the internal mode I crack of length $2l_0$, that is subjected to uniform far-field tensile stresses σ_∞, will be written as [9, 10]

$$\sigma_{xx} = \operatorname{Re} Z_1 - y \operatorname{Im} Z_1',$$

$$\sigma_{yy} = \mathrm{Re}\, Z_1 + y\,\mathrm{Im}\, Z_1', \quad (1)$$
$$\sigma_{xy} = -y\,\mathrm{Re}\, Z_1',\ \sigma_{xz} = \sigma_{yz} = 0,$$
$$\sigma_{zz} = 0 \text{ for the plane stress state,}$$
$$\sigma_{zz} = \nu(\sigma_{xx} + \sigma_{yy}) \text{ for plane strain,}$$

where Z_1 is the holomorphic function in the form

$$Z_1 = \frac{\sigma_\infty}{\pi\sqrt{z^2 - l_0^2}} \int\limits_{-l_0}^{l_0} \frac{\sqrt{l_0^2 - \xi^2}}{z - \xi}\,d\xi$$
$$= \frac{J}{\sqrt{2\pi(z - l_0)}},$$
$$J = \frac{\sqrt{2}\sigma_\infty}{\sqrt{\pi(z + l_0)}} \int\limits_{-l_0}^{l_0} \frac{\sqrt{l_0^2 - \xi^2}}{z - \xi}\,d\xi$$
$$= \frac{\sqrt{2\pi}\sigma_\infty}{\sqrt{(z + l_0)}}(z - \sqrt{z^2 - l_0^2}).$$

The stress field behavior in the neighborhood of the crack tip is studied with the use of the polar system of coordinates:

$z - l_0 = re^{i\theta},\ r = \sqrt{(x - l_0)^2 + y^2},$
$\theta = \mathrm{arctg}[y/(x - l_0)]$ at $x > l_0$,
$\theta = \mathrm{arctg}[y/(x - l_0)] + \pi$ at $x \le l_0$.

Find $\mathrm{Re}\, Z_1$, $\mathrm{Im}\, Z_1$, $\mathrm{Re}\, Z_1'$, $\mathrm{Im}\, Z_1'$, $\mathrm{Re}\, J$, $\mathrm{Im}\, J$, $\mathrm{Re}\, J'$, and $\mathrm{Im}\, J'$ for arbitrary r:

$$\mathrm{Re}\, Z_1 = \frac{1}{\sqrt{2\pi r}}\left(\mathrm{Re}\, J\cos\frac{\theta}{2} + \mathrm{Im}\, J\sin\frac{\theta}{2}\right),$$
$$\mathrm{Im}\, Z_1 = \frac{1}{\sqrt{2\pi r}}\left(-\mathrm{Re}\, J\sin\frac{\theta}{2} + \mathrm{Im}\, J\cos\frac{\theta}{2}\right),$$
$$\mathrm{Re}\, Z_1' = \frac{1}{\sqrt{2\pi r}}\left\{\mathrm{Re}\, J'\cos\frac{\theta}{2} + \mathrm{Im}\, J'\sin\frac{\theta}{2} - \frac{1}{2r}\left(\mathrm{Re}\, J\cos\frac{3\theta}{2} + \mathrm{Im}\, J\sin\frac{3\theta}{2}\right)\right\},$$
$$\mathrm{Im}\, Z_1' = \frac{1}{\sqrt{2\pi r}}\left\{-\mathrm{Re}\, J'\sin\frac{\theta}{2} + \mathrm{Im}\, J'\cos\frac{\theta}{2} + \frac{1}{2r}\left(\mathrm{Re}\, J\sin\frac{3\theta}{2} - \mathrm{Im}\, J\cos\frac{3\theta}{2}\right)\right\},$$
$$\mathrm{Re}\, J = \sqrt{2\pi}\sigma_\infty\left(\frac{r_1}{\sqrt{r_2}}\cos\left[\theta_1 - \frac{\theta_2}{2}\right] - \sqrt{r}\cos\frac{\theta}{2}\right), \quad (2)$$
$$\mathrm{Im}\, J = \sqrt{2\pi}\sigma_\infty\left(\frac{r_1}{\sqrt{r_2}}\sin\left[\theta_1 - \frac{\theta_2}{2}\right] - \sqrt{r}\sin\frac{\theta}{2}\right),$$
$$\mathrm{Re}\, J' = \sqrt{2\pi}\sigma_\infty \times\left(\frac{1}{\sqrt{r_2}}\cos\frac{\theta_2}{2} - \frac{r_1}{2\sqrt{r_2^3}}\cos\left[\theta_1 - \frac{3\theta_2}{2}\right] - \frac{1}{2\sqrt{r}}\cos\frac{\theta}{2}\right),$$
$$\mathrm{Im}\, J' = \sqrt{2\pi}\sigma_\infty \times\left(-\frac{1}{\sqrt{r_2}}\sin\frac{\theta_2}{2} - \frac{r_1}{2\sqrt{r_2^3}}\sin\left[\theta_1 - \frac{3\theta_2}{2}\right] + \frac{1}{2\sqrt{r}}\sin\frac{\theta}{2}\right),$$

where

$$r_1 = \sqrt{x^2 + y^2},\ r_2 = \sqrt{(x + l_0)^2 + y^2},$$
$$\theta_1 = \mathrm{arctg}[y/x],\ \theta_2 = \mathrm{arctg}[y/(x + l_0)].$$

Substitution of (2) into (1) gives

$$\sigma_{xx} = \frac{1}{\sqrt{2\pi r}}\left\{\mathrm{Re}\, J\cos\frac{\theta}{2}\left(1 - \sin\frac{\theta}{2}\sin\frac{3\theta}{2}\right) + \mathrm{Im}\, J\sin\frac{\theta}{2}\left(1 + \cos\frac{\theta}{2}\cos\frac{3\theta}{2}\right) + 2r\left(\mathrm{Re}\, J'\sin^2\frac{\theta}{2}\cos\frac{\theta}{2} - \mathrm{Im}\, J'\cos^2\frac{\theta}{2}\sin\frac{\theta}{2}\right)\right\},$$
$$\sigma_{yy} = \frac{1}{\sqrt{2\pi r}}\left\{\mathrm{Re}\, J\cos\frac{\theta}{2}\left(1 + \sin\frac{\theta}{2}\sin\frac{3\theta}{2}\right) + \mathrm{Im}\, J\sin\frac{\theta}{2}\left(1 - \cos\frac{\theta}{2}\cos\frac{3\theta}{2}\right) - 2r\left(\mathrm{Re}\, J'\sin^2\frac{\theta}{2}\cos\frac{\theta}{2} - \mathrm{Im}\, J'\cos^2\frac{\theta}{2}\sin\frac{\theta}{2}\right)\right\} + \sigma_\infty, \quad (3)$$
$$\sigma_{xy} = \frac{1}{\sqrt{2\pi r}}\left\{\cos\frac{\theta}{2}\sin\frac{\theta}{2}\left(\mathrm{Re}\, J\cos\frac{3\theta}{2} + \mathrm{Im}\, J\sin\frac{3\theta}{2}\right) - 2r\left(\mathrm{Re}\, J'\cos^2\frac{\theta}{2}\sin\frac{\theta}{2} + \mathrm{Im}\, J'\sin^2\frac{\theta}{2}\cos\frac{\theta}{2}\right)\right\},$$
$$\sigma_{zz} = \frac{\nu\sqrt{2}}{\sqrt{\pi r}}\left\{\mathrm{Re}\, J\cos\frac{\theta}{2} + \mathrm{Im}\, J\sin\frac{\theta}{2}\right\} \text{ for plane strain,}$$
$$\sigma_{zz} = 0 \text{ for the plane stress state.}$$

Assuming $y = 0$ in formulae (2) and (3), the following expressions are derived for the plane stress state at $x \ge l_0$ [11]:

$$\sigma_{xx} = \frac{\sigma_\infty x}{\pi\sqrt{x^2 - l_0^2}} - \sigma_\infty,$$
$$\sigma_{yy} = \frac{\sigma_\infty x}{\pi\sqrt{x^2 - l_0^2}},\ \sigma_{xy} = 0. \quad (4)$$

Note that within the classical theory of elasticity the crack tip singularity is obtained.

3. SCHLEICHER YIELD CRITERION

The Schleicher criterion has the form [4, 12]

$$g = \sigma_i + \beta\sigma = \sqrt{2}\tau_*,\ \beta = \mathrm{const}. \quad (5)$$

Here

$$\sigma_i = \sqrt{\sigma'_{ij}\sigma'_{ij}} = \frac{1}{\sqrt{3}}\sqrt{(\sigma_1-\sigma_2)^2+(\sigma_2-\sigma_3)^2+(\sigma_3-\sigma_1)^2},$$

where $\sigma'_{ij} = \sigma_{ij} - 1/3\sigma_{ij}\delta_{ij}$ is the deviatoric stress tensor components and σ_1, σ_2, and σ_3 are the principal stresses (supposing that $\sigma_1 \ge \sigma_2 \ge \sigma_3$) such that

$$\sigma_{1,2} = \frac{\sigma_{xx}+\sigma_{yy}}{2} \pm \sqrt{\left(\frac{\sigma_{xx}-\sigma_{yy}}{2}\right)^2 + \sigma_{xy}^2}, \qquad (6)$$

$\sigma_3 = \nu(\sigma_1+\sigma_2) = \nu(\sigma_{xx}+\sigma_{yy})$ for plane strain,

$\sigma_3 = 0$ for the plane stress state,

where $\sigma = 1/3(\sigma_1+\sigma_2+\sigma_3) = 1/3\sigma_{ii}$ and β is the internal friction coefficient. According to [4], β is of the order of magnitude 0.01. If the tensile and compressive yield stresses σ_t and σ_c are experimentally determined, then [13]

$$\beta = \sqrt{3}\frac{\sigma_c - \sigma_t}{\sigma_c + \sigma_t}.$$

The quantity τ_* is the ultimate pure shear strength of the medium (in case of the Mises criterion $\tau_* = \sigma_c/\sqrt{3}$). Schleicher criterion (5) specifies the Mises yield criterion by considering the influence of the mean normal stress on the critical value of mean tangential stress [14].

By applying the associated flow rule

$$d\varepsilon^p_{ij} = h\frac{\partial g}{\partial \sigma_{ij}}dg \qquad (7)$$

to criterion (5), we derive the following relation:

$$d\varepsilon^p_{ij} = \frac{\sigma'_{ij}}{\sigma_i}hdg + \beta h dg = d\vartheta^p_{ij} + de^p. \qquad (8)$$

The first summand of (8) presents the deviatoric part of plastic strain and is responsible for shape changes. The second summand is in charge of uniform volume variation. By taking the square (in a scalar sense) of the first summand $d\vartheta^p_{ij}$ in (8), obtain

$$d\vartheta^p = \sqrt{d\vartheta^p_{ij}d\vartheta^p_{ij}} = hdg > 0.$$

Thus, as follows from the associated flow rule (7), any plastic deformation should be accompanied not only by shape changes but also by a continuous increase in volume.

The experiments demonstrate the weak influence of σ on the pattern of deformation generation and development. Corrections made to the Schleicher criterion with consideration for σ are, as a rule, of the same order of magnitude as that of internal friction coefficient β (β is of the order of magnitude 0.01). These corrections are usually out of the accuracy of the phenomenological theory of plasticity. However, speaking about cyclic loading, the above corrections are sufficient and comparable with main-order terms. At the symmetric cycle the plastic strain path is expressed by the formula [4]

$$L = 2n\int d\vartheta^p,$$

where n is the number of cycles, L is the length of the "plastic strain path", and the integral is taken within a half cycle. Hence L is proportional to a residual increase in volume and grows in proportion to the cycle number. At rather large n the length L can attain considerable values despite the integral being small. Consequently, the volume can go through significant residual plastic changes $e^p = \beta L$ despite the low coefficient β.

Thus, cyclic loading is a special case, which is most beneficial for such corrections that are made to the yield criterion with consideration for σ in the theory of plasticity. This is explained by the fact that the main terms of the solution remain always restricted by certain limits while correction terms increase continuously in proportion to the number of cycles.

4. ESTIMATE OF THE PLASTIC ZONE BOUNDARY

By substituting formulae (3) describing the stress state at an arbitrary point of the cracked plate into (5), let us write the Schleicher criterion for plane strain as

$$3\frac{\sigma_{xy}^2}{\sigma_\infty^2} + \frac{3}{4}\left(\frac{\sigma_{xx}}{\sigma_\infty} - \frac{\sigma_{yy}}{\sigma_\infty}\right)^2 + \left\{\left(\frac{1}{2}-\nu\right)^2 - \frac{\beta^2}{3}(1+\nu)^2\right\} \times \left(\frac{\sigma_{xx}}{\sigma_\infty} - \frac{\sigma_{yy}}{\sigma_\infty}\right)^2 + \frac{2\sqrt{6}}{3}\beta(1+\nu) \times \left(\frac{\sigma_{xx}}{\sigma_\infty} + \frac{\sigma_{yy}}{\sigma_\infty}\right)\frac{\sigma_c}{\sigma_\infty} = 2\frac{\sigma_c^2}{\sigma_\infty^2}. \qquad (9)$$

Criterion (5) for the plane stress state can be derived if ν is excluded from expression (9), assuming $\nu = 0$.

Figures 2a and 2b show plastic zone boundaries defined by equality (9) for plane strain and plane stress state, respectively ($x_1 = x/l_0$, $y_1 = y/l_0$). Curves *1* and *2* in Fig. 2 are built without consideration for plastic expansion of the material at $\beta = 0$: curves *1* in Fig. 2 correspond to $\sigma_c/\sigma_\infty = 2$ and curves *2* to $\sigma_c/\sigma_\infty = 3$. Curves *1′* and *2′* in Fig. 2 are constructed with consideration for plastic expansion: curves *1′* and *2′* in Fig. 2a correspond to $\beta = 0.01$ while curves *1′* and *2′* in Fig. 2b to $\beta = 0.03$. Note that the presence of mean normal stress σ in the

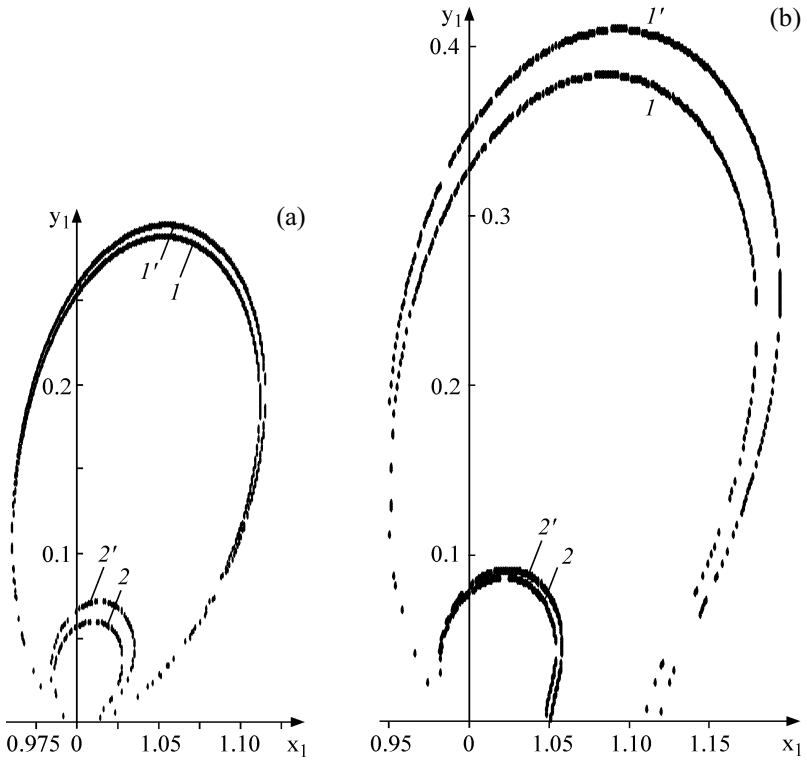

Fig. 2. Plastic zone configurations obtained from the Schleicher criterion for (a) plane strain and (b) plane stress state at $\nu = 1/3$.

Schleicher criterion (5) ensures uniform expansion of the plastic zone.

Plane strain and plane stress state differ in size and shape of the plastic zone. Under plane deformation plastic flow in the crack tip is retarded on account of the effective yield stress being much higher than the yield stress in uniaxial tension. Yield stresses under plane strain and plain stress state are inconstant. Their variation is controlled by the constraint ratio for plastic strain $\chi = \sigma_{max}/\sigma_c$ in such a way that the yield stresses are determined by effective stress $\sigma_{ef} = \chi\sigma_c$. Note that Fig. 2a shows plastic zone boundaries for plane strain at $\chi = 1$. At $\chi > 1$ the plastic zone is less than that marked in Fig. 2a.

5. YIELD STRESS AFFECTED BY PLASTIC LOOSENING FOR PLANE STRAIN AND PLANE STRESS STATE

The combined stress state can usually be represented by principal stresses σ_1, σ_2, and σ_3. The highest of them is σ_1. Use dependences (2), (3), (6), and (9) and suppose $\theta = \theta_1 = \theta_2 = 0$. Express stresses σ_2 and σ_3 in the form

$$\frac{\sigma_2}{\sigma_\infty} = \frac{\sigma_1}{\sigma_\infty} - 1, \quad \frac{\sigma_3}{\sigma_\infty} = \nu\left(2\frac{\sigma_1}{\sigma_\infty} - 1\right), \tag{10}$$

where $\sigma_\infty/\sigma_1 = (\sqrt{x^2-1})/x = t$. Using Schleicher criterion (5), write the constraint ratio for plane strain

$$\chi = \frac{\sigma_1}{\sigma_c} = \sqrt{6}[\sqrt{6}(t^2(\nu^2 - \nu + 1) - t(4\nu^2 - 4\nu + 1) + 4\nu^2 - 4\nu + 1)^{1/2} + \beta(\nu + 1)(2 - t)]^{-1} \tag{11}$$

and the plane stress state

$$\chi = \frac{\sigma_1}{\sigma_c} = \frac{\sqrt{6}}{\sqrt{6}\sqrt{t^2 - t + 1} + \beta(2 - t)}. \tag{12}$$

According to (11) and (12), the higher is the internal friction coefficient, the lower are the constraint ratio and effective stress σ_{ef}. In Fig. 3 curves *1*, *2*, and *3* are built at $\beta = 0$, 0.01 and 0.05, respectively. The constraint ratio χ decreases with distance from the crack tip. In the crack tip, when $x_1 = 1$, $t = 0$, and $\nu = 1/2$, the quantity χ takes on an infinite value. This can be caused by the presence of the crack tip singularity as even in the next step $h = 0.0001$ and $x = 1 + h$ χ possesses a finite value shown in Fig. 3. At point $x_1 = 1$, i.e., on the crack edge being the free surface of a body, the stress state is thought to lack triaxiality [9]. Therefore at $x_1 = 1$ the constraint ratio $\chi = 1$. Thus, on achieving the yield stress σ_c in the crack tip in uniaxial tension, the effective stress rises sharply

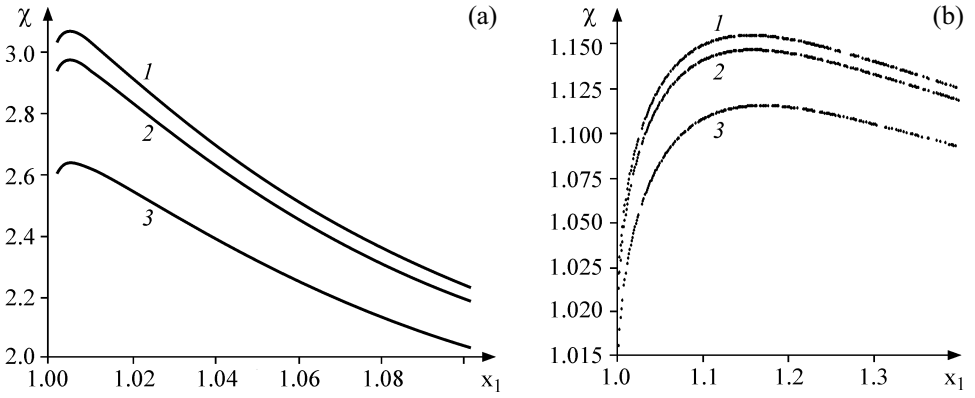

Fig. 3. Constraint ratio variation with distance from the crack tip for (a) plane strain and (b) plane stress state.

up to $\sigma_{ef} = \chi\sigma_c$ [15] and afterwards decreases continuously.

The similar pattern is observed for the plane strain state, with the only difference that there are neither a sharp increase in the small neighborhood of the crack tip nor a sudden drop with distance from it and the effective stress is close to the yield stress.

6. PLASTIC ZONE LENGTH AT $Y = 0$

Let us give an estimate to the longitudinal size of the plastic zone x_1 at $y_1 = 0$. From expression (9) we obtain

$$x_1 = \frac{t_1}{\sqrt{t_1^2 - 1}} - 1, \qquad (13)$$

where

$$t_1 = 1 - \frac{A_2}{2A_1} + \frac{\sqrt{A_2^2 - 4A_1A_3}}{2A_1},$$

$$A_1 = 6(1-2\nu)^2 - 4\beta^2(1+\nu),$$

$$A_2 = 6(1-2\nu)^2 + 12\sqrt{2}\beta(1+\nu)\frac{\tau_*}{\sigma_\infty} - 4\beta^2(1+\nu),$$

$$A_3 = 6(\nu^2 - \nu + 1) - \beta^2(1+\nu) + 6\sqrt{2}\beta(1+\nu)\frac{\tau_*}{\sigma_\infty} - 18\frac{\tau_*^2}{\sigma_\infty^2}.$$

Not taking into account the smooth part (stress σ_∞) in formula (3) derived for normal stress σ_{yy} and studying only the asymptotic behavior of stress near the crack tip $\rho \ll l_0$, formula (13) for plane strain can be replaced by the following approximate equality [9]:

$$r(\theta) \cong \frac{K_I^2}{4\pi\sigma_c^2}\left[\frac{3}{2}\sin^2\theta + (1-2\nu)^2(1+\cos\theta)\right], \qquad (14)$$

where $r(\theta)$ is the dimensionless radius-vector and $K_I = \sigma_\infty\sqrt{\pi l_0}$ is the stress intensity coefficient.

Under high stresses in the vicinity of the crack tip the Poisson's ratio ν varies and tends to $1/2$. In this case, according to the approximate formula (14), at $\theta = 0$ and $\nu = 1/2$ the plastic zone length in front of the crack tip is $r(\theta) = 0$. Consequently, at $\nu = 1/2$ in the plastic zone in a line with the crack the material is not subjected to plastic deformation. The statement made in paper [16] allows formulating the hypothesis of the transition of a thin material layer along a line of the crack extension at $\nu = 1/2$ to the condition of incompressibility.

Figure 4 demonstrates dependence (13) with (curve *1*, $\beta = 0.05$) and without consideration (curve *2*, $\beta = 0$) for plastic expansion. According to Fig. 4, the plastic zone length x_1 ahead the crack at different σ_c/σ_∞ takes nonzero values ($x_1 \to 0$ only at $\sigma_\infty \to 0$). Consequently, the assumption on the impossibility of plastic zone formation at $\theta = 0$ and $\nu = 1/2$ that follows from the approximate equality (14) is groundless. An inherent error underlies it.

7. STRAIN-DEPENDENT VARIATION IN POISSON'S RATIO

Let us rewrite Schleicher yield criterion (5) at y_1 in the form

$$B_1\nu^2 + B_2\nu + B_3 = 0, \qquad (15)$$

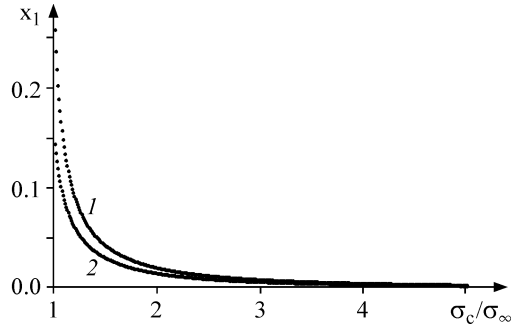

Fig. 4. Plastic zone length x_1 at $y_1 = 0$ versus far-field load σ_∞ at $\beta = (1)\ 0.05$ and $(2)\ 0$.

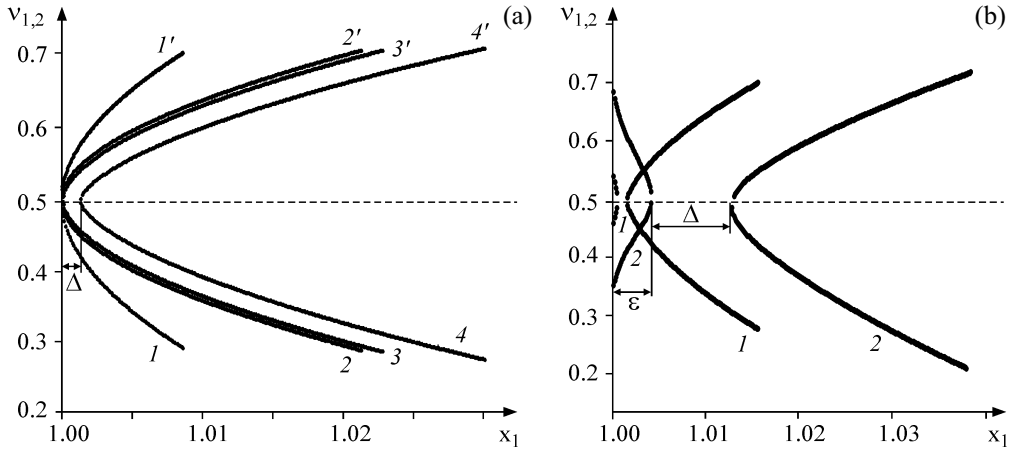

Fig. 5. Poisson's ratio variation in the plastic zone in a line with the crack.

where

$$B_1 = (2t_1 + 1)^2 (6 - \beta^2),$$

$$B_2 = -2(2t_1 + 1)^2 (3 + \beta^2) + 6\sqrt{2}\beta(2t_1 + 1)\frac{\tau_*}{\sigma_\infty},$$

$$B_3 = 6(t_1^2 + t_1 + 1) - \beta^2(2t_1 + 1)^2 + 6\sqrt{2}\beta(2t_1 + 1)\frac{\tau_*}{\sigma_\infty} - 18\frac{\tau_*^2}{\sigma_\infty^2},$$

$$t_1 = \frac{x}{\sqrt{x^2 - 1}}.$$

The roots of equation (15) are

$$\nu_{1,2} = \frac{-B_2 \pm \sqrt{B_2^2 - 4B_1B_3}}{2B_1}, \ \nu_2 > \nu_1. \qquad (16)$$

Figure 5a for different σ_c/σ_∞ and β illustrates two solutions (16) of equation (15): ν_1 (curves *1–4*) and ν_2 (curves *1′–4′*). The solutions are separated by a dashed line. Consideration is given only to descending branches corresponding to the ν_1 root. Curves *1* and *2* are built at $\beta = 0$ and $\sigma_c/\sigma_\infty = 3$ and 2, respectively, while curves *3* and *4* at $\sigma_c/\sigma_\infty = 2$ and $\beta = 0.01$ and 0.05, respectively. In the immediate vicinity of the crack tip the Poisson's ratio $\nu_1 \approx 1/2$ and ν_1 decreases with distance from it until taking a value typical of a plastically undeformed material. At plastic expansion the Poisson's ratio decreases more slowly.

In Fig. 5b curves *1* and *2* are built at $\sigma_c/\sigma_\infty = 3$ and $\beta = 0.05$ and 0.1, respectively. Similarly to Fig. 5a consideration is given only to descending branches corresponding to the ν_1 root of equation (15). The figure demonstrates the interval Δ, where equation (15) has no solutions. The higher is β, the wider is Δ. At low β (see curve *4* in Fig. 5a built at $\beta = 0.01$) the interval Δ is also observed. With increasing β the interval Δ shifts to the right with respect to the tip. The Poisson's ratio in Fig. 5b grows to $1/2$ on the interval $1 < x_1 < 1 + \varepsilon$ and decreases on the interval $1 + \varepsilon + \Delta < x_1 < 1 + \Delta_p$ (Δ_p is the plastic zone length). The lack of solutions on the interval Δ is evidently related to the fact that yield criterion (5) is inoperative on this interval due to lack of plasticity itself. Note that the stepwise propagation of fatigue cracks is associated with exhausted plasticity in a certain small neighborhood of the crack tip whose size is determined by several lattice parameters. For example, in case of steel specimens the crack propagation step comprises 4 μm at the cycle number $n = 10^4$ and stress amplitude 90 MPa [16, 17]. In turn, the plasticity exhaustion is accompanied by the formation of dislocation cell structure that governs the micropore formation, i.e., material loosening. The region of exhausted plasticity in front of the crack tip is experimentally stated to be shorter than the plastic zone. After the critical number of cycles the crack demonstrates a brittle microstep over the whole region of exhausted plasticity. The material within this region is supposed to be incompressible [16]. The region of exhausted plasticity is probably equal to the interval Δ in length. In this case the internal friction coefficient β is likely inconstant as it peaks in the small neighborhood of the crack tip and decreases with distance from it. Note that the cell structure changes continuously during cyclic loading thus inducing autowave processes [18, 19]. Under their action such material parameters as Poisson's ratio, loosening coefficient, constraint ratio for plastic strain, etc., should also change continuously.

Thus, the mean normal stress σ in the Schleicher criterion ensures uniform expansion of the plastic zone. In this case the plastic zone is inhomogeneous, i.e., the ma-

terial characteristics, such as Poisson's ratio, constraint ratio for plastic strain (and possibly others) are inconstant. They decrease with distance from stress concentrators and peak in the defect tip or in the immediate vicinity of it. Though the experiments point to a rather weak influence of σ on the pattern of deformation formation and development, as far as cyclic loading is concerned, the given corrections are significant and comparable to main-order terms.

The paper has studied only a small amount of changes occurring in the material under plastic deformation. The developed multilevel model of a deformable solid considers plastic flow of a solid as irreversible self-consistent changes in related functional systems and describes mathematically this process on all scales.

The work is performed at the financial support of RFBR (Grant Nos. 10-08-00220 and 11-08-00191).

REFERENCES

1. Panin, V.E. and Egorushkin, V.E., Nonequilibrium Thermodynamics of a Deformed Solid as a Multiscale System. Corpuscular-Wave Dualism of Plastic Shear, *Phys. Mesomech*., 2008, vol. 11, no. 3–4, pp. 105–123.
2. Rybin, V.V., *Severe Plastic Deformation and Fracture of Metals*, Moscow: Metallurgiya, 1986.
3. Panin, V.E., Elsukova, T.F., Egorushkin, V.E., Vaulina, O.Yu., and Pochivalov, Yu.I., Nonlinear Wave Effects of Curvature Solitons in Surface Layers of High-Purity Aluminum Polycrystals under Severe Plastic Deformation. I. Experiment, *Phys. Mesomech.*, 2008, vol. 11, no. 1–2, pp. 63–72.
4. Novozhilov, V.V., On Plastic Loosening, *Prikl. Mat. Mekh*., 1965, vol. 29, no. 4, pp. 681–689.
5. Stang, A.H., Greenspan, M., and Newman, S.B., Poisson's Ratio of Some Structural Alloys for Large Strains, *J. Res. Nat. Bur. Stand*, 1946, vol. 37, no. 4, pp. 211–221.
6. Davidenkov, N.N. and Vasil'eva, D.M., On Poisson's Ratio, *Zavod. Lab.*, 1952, vol. 18, no. 5, pp. 596–599.
7. Zhukov, A.M., On Poisson's Ratio in Plastic Zone, *Izv. Akad. Nauk SSSR. Otdel. Tekhn. Nauk*, 1954, no. 12, pp. 86–91.
8. Bolshanina, M.A. and Panin, V.E., Latent Energy of Deformation, in *Investigation of Physics of Deformation*, Izv. Akad. Nauk SSSR, 1957, pp. 193–233.
9. Kershtein, I.M., Klyushnikov, V.D., Lomakin, E.V., and Shesterikov, S.A., *Fundamentals of Experimental Fracture Mechanics*, Moscow: Mosk. Univ., 1989.
10. Kozhevnikova, M.E., Refinement of the Plastic-Zone Boundary in the Vicinity of a Crack Tip for the Quasiviscous and Viscous Types of Fracture, *J. Appl. Mech. Tech. Phys.*, 2005, vol. 46, no. 1, pp. 102–107.
11. Hellan, K., *Introduction to Fracture Mechanics*, New York: McGraw-Hill, 1984.
12. Novozhilov, V.V., On Physical Sense of Stress Invariants in the Theory of Plasticity, *Prikl. Mat. Mekh.*, 1952, vol. 16, no. 5, pp. 615–619.
13. Kovrizhnykh, A.M., Plane Stress Equations for the Von Mises–Schleicher Yield Criterion, *J. Appl. Mech. Tech. Phys.*, 2004, vol. 45, no. 6, pp. 894–901.
14. Kadashevich, Yu.I. and Novozhilov, V.V., Theory of Plasticity Taking into Account Residual Microstresses, *Prikl. Mat. Mekh.,* 1958, vol. 22, no. 1, pp. 78–89.
15. Shiratori, M., Miyoshi, T., and Matsushita, H., *Numerical Fracture Mechanics*, Tokyo: Jikkyo Shuppan, 1980.
16. Arutyunyan, R.A., *Problems of Strain Aging and Long-Term Fracture in Mechanics of Materials*, Saint-Petersburg: Izd. St.-Petersb. Univ., 2004.
17. Ivanova, V.S. and Terentiev, V.F., *Nature of Fatigue of Metals*, Moscow: Metallurgiya, 1975.
18. Zuev, L.B. and Danilov, V.I., Slow Autowave Processes in Deformed Solids, *Phys. Mesomech.*, 2002, vol. 5, no. 5–6, pp. 97–114.
19. Zuev, L.B. and Danilov, V.I., The Nature of Large-Scale Correlations in Plastic Flow, *Phys. Solid State*, 1997, vol. 39, no. 8, pp. 1241–1245.